sustainability

MDPI

Article

Projection of Thermal Bioclimate of Egypt for the Paris Agreement Goals

Mohammed Magdy Hamed [1,2], Mohamed Salem Nashwan [3,*], Tarmizi bin Ismail [2] and Shamsuddin Shahid [2,*]

[1] Construction and Building Engineering Department, College of Engineering and Technology, Arab Academy for Science, Technology and Maritime Transport (AASTMT), B 2401 Smart Village, Giza 12577, Egypt
[2] Department of Water & Environmental Engineering, School of Civil Engineering, Faculty of Engineering, Universiti Teknologi Malaysia, Skudai 81310, Johor, Malaysia
[3] Construction and Building Engineering Department, College of Engineering and Technology, Arab Academy for Science, Technology and Maritime Transport (AASTMT), 2033 Elhorria, Cairo 11736, Egypt
* Correspondence: m.salem@aast.edu (M.S.N.); sshahid@utm.my (S.S.)

Abstract: This paper presents the likely changes in the thermal bioclimate of Egypt under the Paris Agreement, which aimed to restrict global warming to increase by 1.5–2.0 °C. A mean multi-model ensemble (MME) of eight global climate models were employed to evaluate the two shared socioeconomic paths (SSP) scenarios SSP1-1.9 and SSP1-2.6, which indicated scenarios for 1.5 and 2.0 °C rates of warming, respectively. The spatial distribution of the observed bioclimate indicated higher values in the south and southeast regions. The findings showed that there was an increase in Egypt's mean temperature by rates of 1.3 and 1.5 °C for SSP1-1.9 and SSP1-2.6, respectively, with a higher increase in the southeast. The SSP1-2.6 scenario showed a gradual temperature rise with time, while SSP1-1.9 projected a decrease in the far future. The daily temperature variation decreased in the same region, but this effect was amplified in the north by 0.2 °C. The seasonality decreased by −0.8 to −2.3% without any shift in isothermality. The maximum summer temperature increased more (1.3–2.2 °C) than the minimum winter temperature (0.9–1.5 °C), causing an increase in inter-seasonal variability. Most bioclimatic indicators more rapidly rose in the north and northeast regions of Egypt, according to the geographical distribution of their projections.

Keywords: Paris Agreement; bioclimatic; CMIP6; SSP; climate change

Citation: Hamed, M.M.; Nashwan, M.S.; Ismail, T.b.; Shahid, S. Projection of Thermal Bioclimate of Egypt for the Paris Agreement Goals. *Sustainability* **2022**, *14*, 13259. https://doi.org/10.3390/su142013259

Academic Editor: Mohammad Aslam Khan Khalil

Received: 26 September 2022
Accepted: 13 October 2022
Published: 15 October 2022

1. Introduction

A bioclimate affects a region's species distribution, plant cover, ecology, irrigation requirements, and vulnerability to climate hazards, among other factors [1,2]. As a result, understanding the bioclimate of a region is valuable for understanding how climate affects living creatures on an annual and seasonal basis [3]. This information includes the mean values, standard deviations, inter- and intra-annual variability, and seasonality of the thermal environment. Climate factors such as temperature, humidity, and wind speed significantly affect human comfort and energy levels [4,5]. Consequently, mapping the spread of human comfort zones using thermal bioclimatic indicators provides valuable information [6,7]. The indicators can help assess a region's suitability for cultivating a specific crop type [8].

Many climatic features associated with a biosphere have shifted due to climate change [9–11]. The bioclimate is sensitive to minor changes in the climate; therefore, climate change can significantly affect the biological distribution [12–15]. It may also lead to a change in the species distribution and ecology of a region [16,17]. Climate changes affect many climate variables (e.g., temperatures, precipitations, etc.) and their characteristics, such as seasonality and intra-annul variability [4,18,19]. These have also altered the environmental risks to human health and the biological habitat. Therefore, bioclimatic

indicators have been increasingly assessed to understand climate change effects on bioenvironments [20–22]. Knowing the changes in bioclimate is also quite beneficial for climate change adaptation and sustainable bioenvironment management [11,23].

Human-caused greenhouse gases (GHG) emissions and land-use changes will continue to impact climate in the future. Simulating Earth's climatic reaction to GHG emissions and land-use changes requires global climate models (GCMs) [24–26]. These GCMs are being released as part of the phases of the Coupled Model Intercomparison Project (CMIP). The most recent project (CMIP6) differs from previous CMIPs as it incorporates much more reliable Earth processes [27,28]. Moreover, the models project climate for different scenarios that are labelled as shared socioeconomic pathways (SSPs). Two SSPs (SSP1-1.9 and SSP1-2.6) address the Paris Agreement's goals of controlling global warming to only a 1.5 and 2.0 °C increase above the pre-industrial era [29,30]. SSP1-1.9 demonstrates the scenario where CO_2 emissions would net zero around 2050, which is the most optimistic scenario. This transition caused a shift in societal attention from economic growth to total well-being. This scenario would limit warming to around 1.5 °C above pre-industrial, dipping back to 1.4 °C by 2100. SSP1-2.6 is the second most optimistic scenario, which projects CO_2 emission reduction at a slower rate than in SSP1-1.9; it projects a steady rise in global warming until it reaches 1.8 °C by 2100.

Egypt has a unique biogeographical characteristic due to its location at the heart of the great Saharo-Sindian desert belt. It is also the intersection of four biogeographical regions: the Mediterranean, Afrotropical, Irano-Turanian, and Saharo-Sindian. In addition, it includes six biogeographical sectors (Figure 1), including the Libo-Nubian, Nilotic, Marioutico-Arishian, Sinaico-Arabian, Elbanian, and Suezian sectors [31]. Additionally, the Nile River penetrates the country from south to north. The Red Sea and Mediterranean Sea are linked by the Suez Canal, which has a long-term impact on the biotic diversity [32–34]. Egypt is home to highly diverse terrestrial habitats, flora, and fauna compositions. However, due to the arid and hyper-arid climates, a few species with some endemic species can be found [35,36]. Recent changes in land-use [37], pollutants [38,39], and human activities [40,41] have affected the biodiversity of several locations in Egypt.

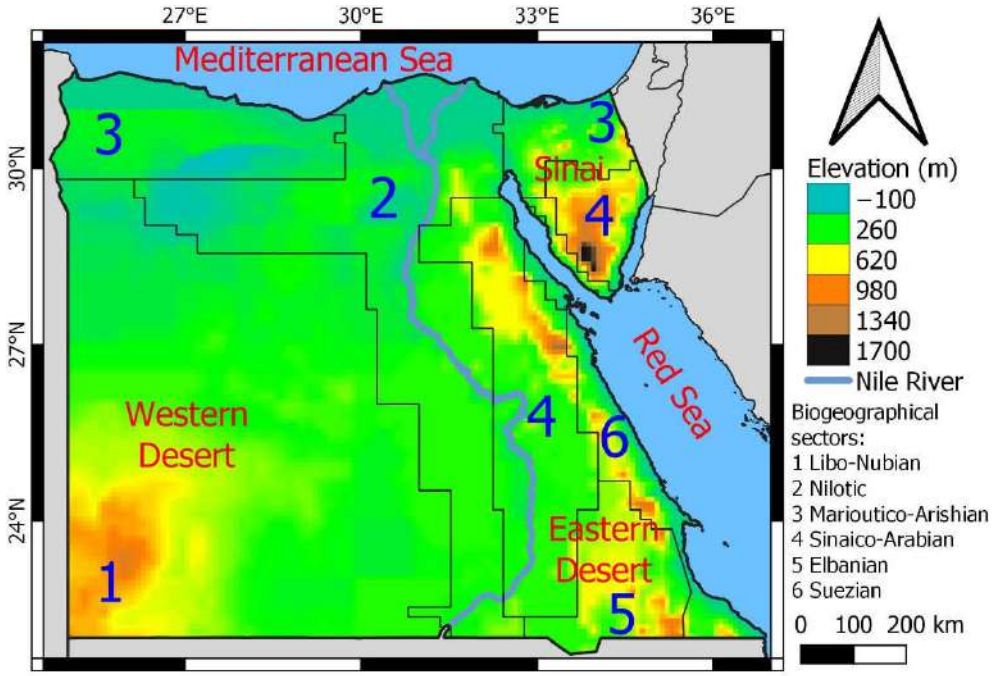

Figure 1. The Egyptian topography.

This study aims to quantify the bioclimate change in Egypt over time for the most optimistic scenarios of limiting global warming according to the Paris Agreement. Eleven

thermal bioclimatic indicators were projected for SSP1-1.9 and SSP1-2.6 using eight CMIP6 GCMs. The projections of the bioclimates would help ecologists and biologists to extend the research on climate change responses to species. Furthermore, it can aid policymakers in formulating climate change mitigation and adaptation policies for Egypt.

2. Research Area and Climate Data

2.1. Egypt

Egypt (21.7° N–31.7° N and 24.7° E–35.8° E) is a northeast African country with a population above 100 million and an area of approximately one million km^2. Egypt's terrain is almost flat, excluding the eastern Red Sea and Sinai Mountains, northern Qattara Depression, and southwestern Al Jelf Alkabir Plateau (Figure 1). Egypt has an arid climate with an annual precipitation of nearly 200 mm in the north and below 5 mm in the southern desert, respectively [42,43]. The average Tmax and Tmin are 27.7 and 15.8 °C; the south is relatively hotter than the north.

2.2. Climate Data

This study employed CMIP6 GCMs to evaluate the likely changes in the thermal bioclimates of Egypt. Eight different GCMs were used, and are listed in the first table (Table S1) in Supplementary Materials. They all shared a common initial variant label, r1i1p1f1. The outputs of the GCMs (e.g., monthly accumulative precipitation and monthly mean Tmax and Tmin) that were used were the historical (1975–2014) and future simulations (2020–2099) under SSP1-1.9 and SSP1-2.6, which address the Paris Agreement's goal. SSP1-1.9 simulates the climate considering a global warming of lower than 1.5 °C at 2100, following a mild increase (1.6 °C) at the mid-century. This scenario utilizes SSP1, which models a sustainable choice for Earth's future development; it represents the most optimistic scenario. SSP1-2.6 shares the same SSP, but has higher Representative Concentration Pathways (RCP) (2.6 W/m^2) that considers global warming being limited to 1.8 °C at the end of the century. To eliminate any potential for bias in geographical representation, the results of both the historical and future GCMs were interpolated to a resolution of 100 km × 100 km.

3. Methodology

The climatic and bioclimatic changes are very diverse among locations. The fast increase in global temperature mainly affects the thermal bioclimates. Consequently, thermal indicator changes must be urgently addressed. Climate change may be more effectively monitored using bioclimatic markers. In light of the global warming objectives established by the Paris Agreement, our analysis assessed how the future thermal bioclimatic indices in Egypt will shift. Eleven thermal bioclimatic indicators (Table S2 in Supplementary Materials) were adopted to address this aim, as listed in the Results subsections.

Bioclimatic indicators were computed using the climatic variables (rainfall, Tmax, and Tmin) derived from the GCM simulations. The eight GCM outputs were used to create a mean MME, which was utilized to calculate the bioclimatic indicators for the historical (1975–2014) and two future periods, near (2020–2059) and far (2060–2099). Each thermal bioclimatic indicator's historical status was presented using the respective MME mean. The projected changes in the MME in the two future periods compared with the historical MME were computed to show the spatial distributions of the changes. The primary goal of the MME mean is to reduce uncertainty in future simulations and accurately represent climate change [44–46]. The changes in bioclimatic indicators were calculated at each grid to create maps of the projected changes in the indicators for different periods.

4. Results

4.1. Annual Mean Temperature (Bio-1)

Figure 2 shows the Bio-1 distribution in Egypt. The Bio-1 ranged between 20.5 °C in the northwest and 24.5 °C in the southeast. There is a steady rise in the mean temperature

(Tmean) from the north to the south. The projections of Bio-1 showed a rise of 1.1–1.7 °C. The projected near future change ranged between 1.2 °C and 1.6 °C; in the 2060–2099 range, the increase was projected to be between 1.1 and 1.7 °C. The changes are lower during the 2060–2099 period compared with the 2020–2059 range for the SSP1-1.9 scenario. In contrast, the changes are higher for the 2060–2099 range compared with the 2020–2059 range for the SSP1-2.6 scenario.

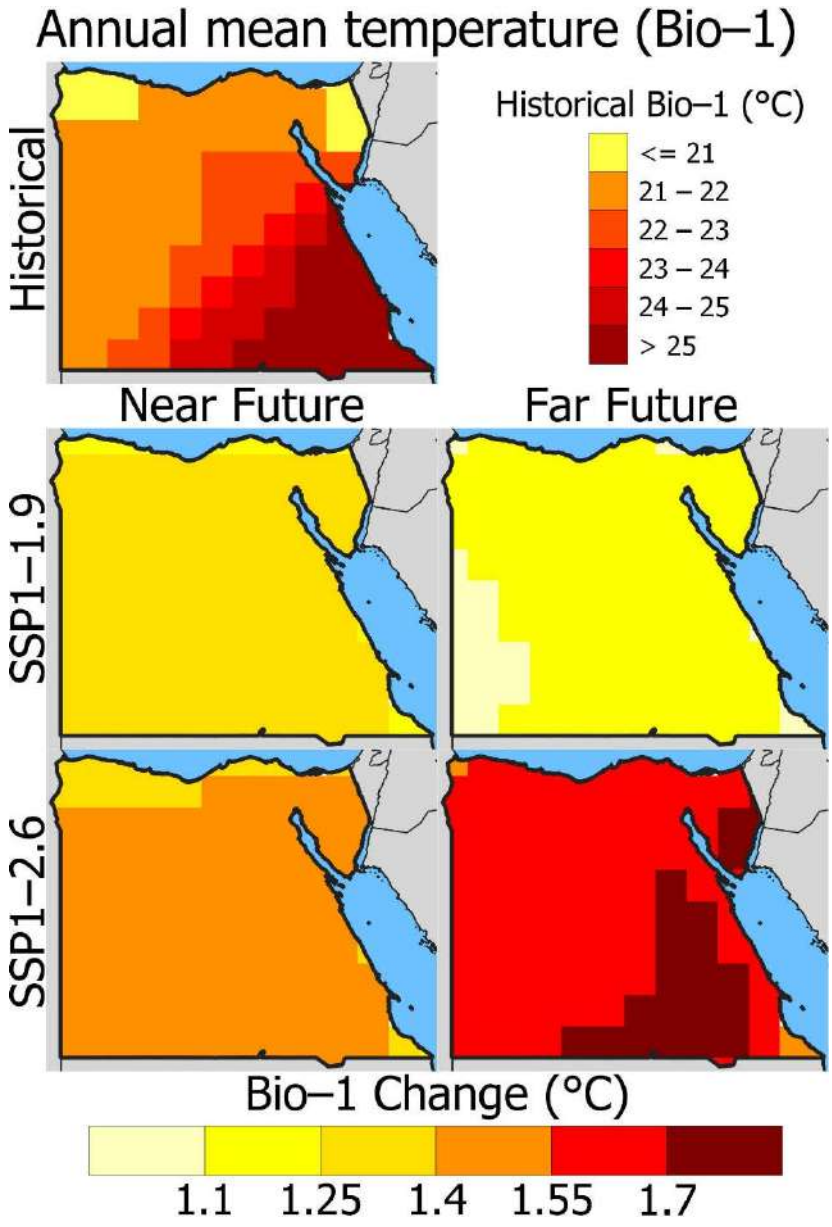

Figure 2. Maps of the mean changes (°C) in Bio-1 in the near and far future periods for SSP1-1.9 and SSP1-2.6 compared with the reference period.

4.2. Diurnal Temperature Range (Bio-2)

Bio-2 is the daily variation between the Tmax and Tmin, which significantly impacts ecosystems. The lesser influence of the local climate on Bio-2 has made it a good indicator of climate change for global warming [47]. According to some research, Tmin has significantly increased above Tmax, decreasing the Bio-2 in various places [47,48]. On a global scale, this phenomenon has been linked to climate change. The Bio-2 (Figure 3) of Egypt showed a wide variation across the region, ranging from 6.0 to 19.0 °C. However, the projected changes of this indicator were very low, ranging between −0.1 °C and 0.2 °C. The changes

were positive in the north and negative in the south for both SSPs. The increase was larger in the far future, particularly in the northern regions.

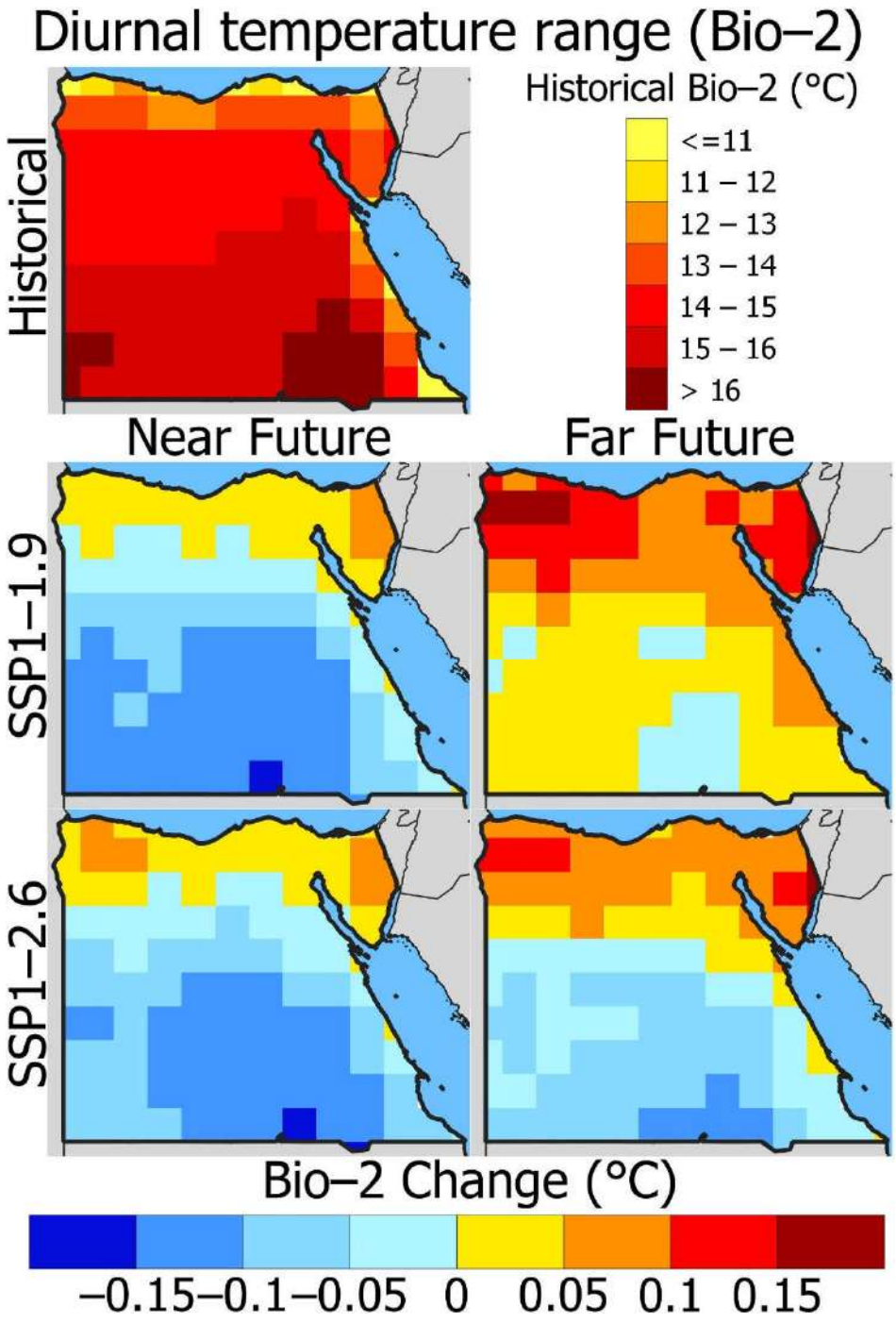

Figure 3. Same as Figure 2, but for Bio-2.

4.3. Isothermality (Bio-3)

Bio-3 is regarded as an essential indicator in tropical and coastal locations as it is the proportion of Bio-2 (daytime temperature spread) to Bio-7 (yearly temperature spread) [49]. A low Bio-3 value suggests a lesser variability in the daily temperature than in the yearly; it can range from 0 to 100%. Figure 4 depicts the geographical variability of Bio-3 in Egypt during the reference period, along with the shifts for the future periods. The Bio-3 ranged between 31.0 and 44.0% in Egypt. The lowest values were found in the coastal regions,

especially along the Red Sea. The Bio-3 was projected to decrease for both scenario models and future periods. However, the change would be very small (0 to −0.7%), indicating a minimal influence of climate change on isothermality. Additionally, the changes were projected to be lower for the far future period, indicating no change in isothermality if global warming can be limited according to the Paris Agreement.

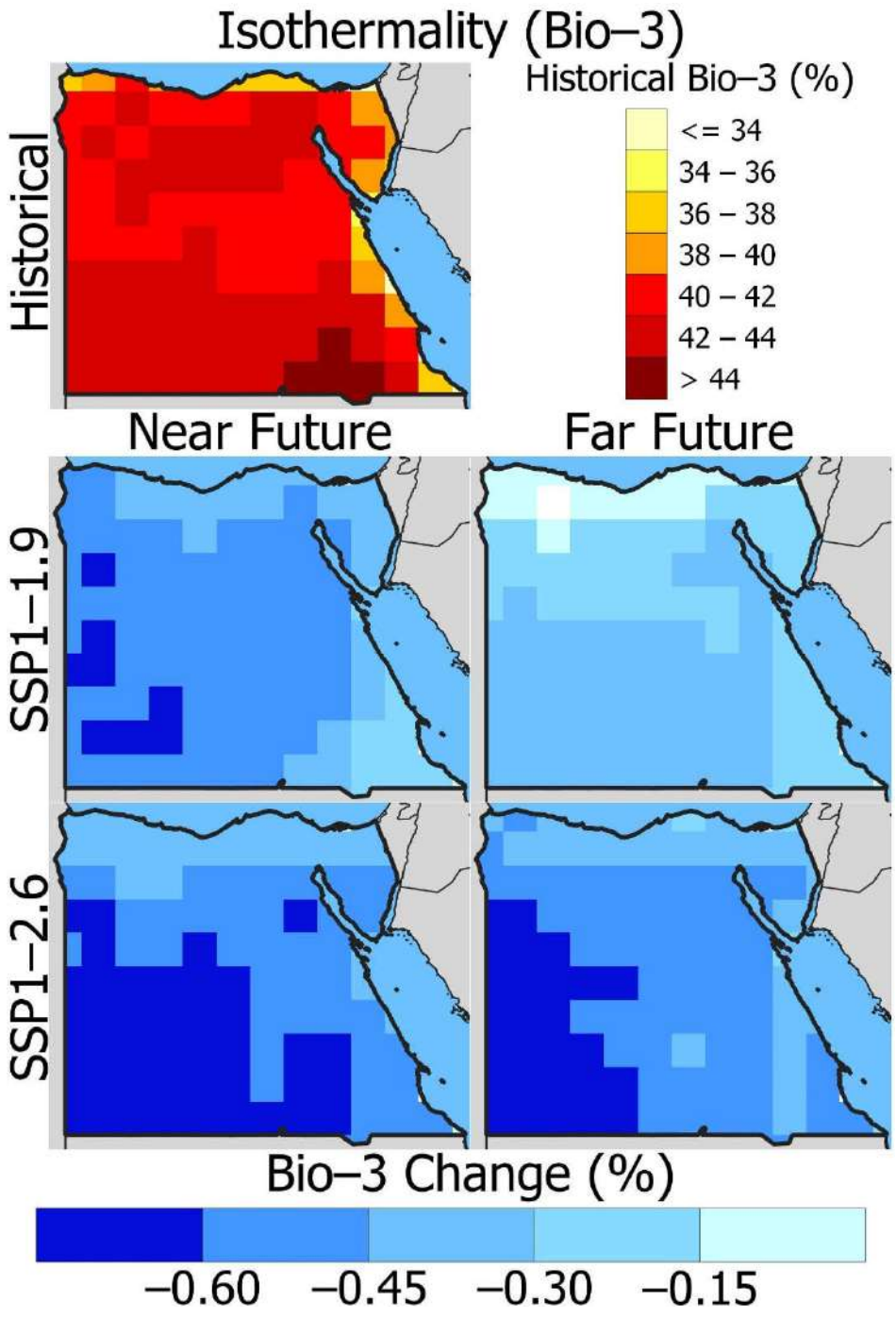

Figure 4. Same as Figure 2, but for Bio-3.

4.4. Temperature Seasonality (Bio-4)

Figure 5 describes the geographical variability of the historical and future shifts in Bio-4 across Egypt. The greater the seasonality, the greater the percentage change in temperature over a year, indicating a greater temperature fluctuation, and vice versa [3]. The Bio-4 ranged between 26.0% in the southeast and 39.0% in the northeast. The analysis

showed that the future changes ranged between −0.8 and −2.3% for the different SSPs and periods. The average deviations were −1.3 and −1.7% for SSP1-1.9 and 1-2.6, respectively. The region with the lower Bio-4 will likely experience a smaller shift and vice versa for both SSPs. This indicates the future spatial heterogeneity in Bio-4 due to climate change.

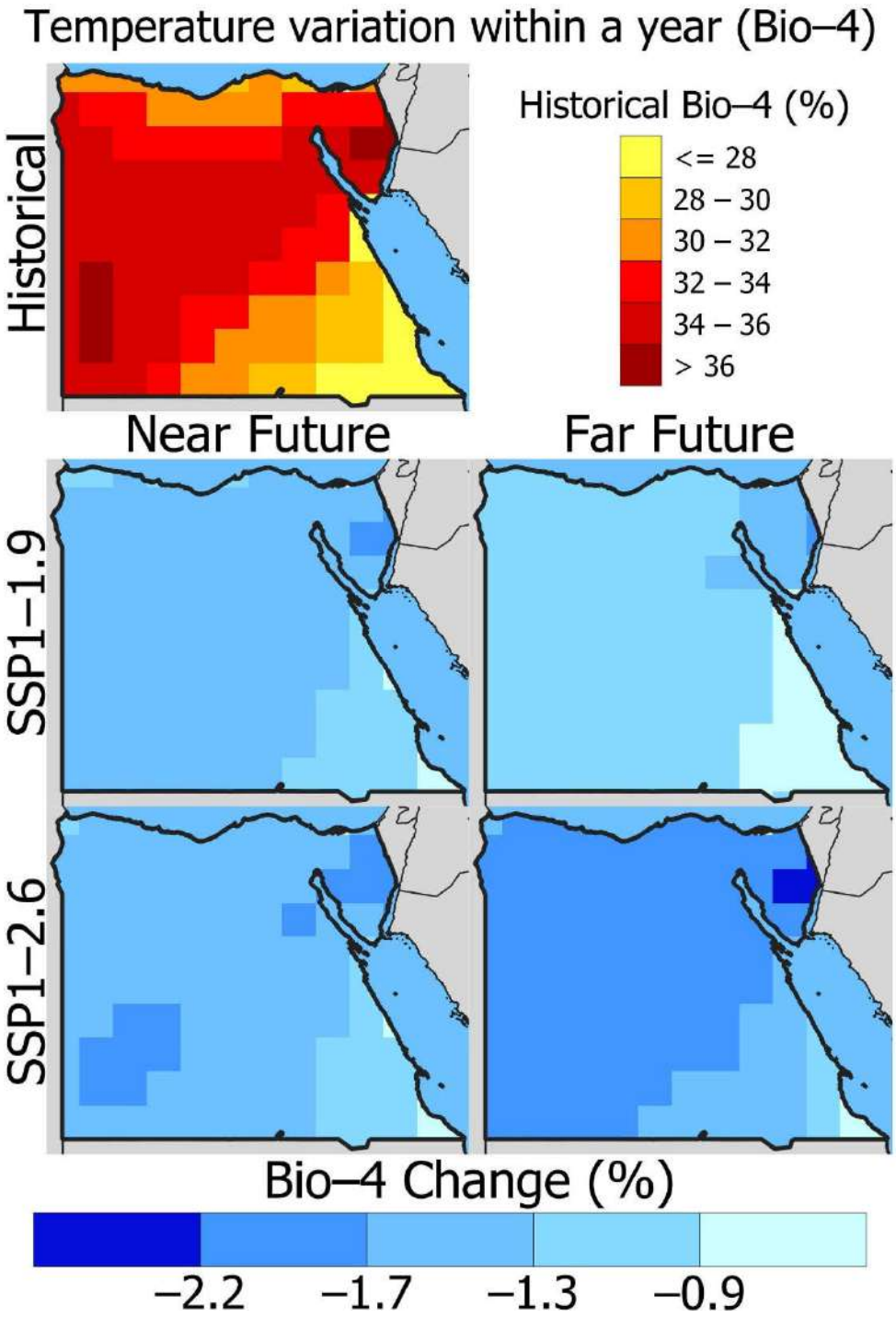

Figure 5. Same as Figure 2, but for Bio-4.

4.5. Tmax in the Hottest Month (Bio-5)

Figure 6 depicts the warmest monthly temperature (Bio-5) for Egypt's historical and climate change scenarios. The Bio-5 varied between 36.0 and 43.0 °C. The minimum was in the Mediterranean (36.5 °C) region, while the highest value was in the southeast region.

The temperature rise was projected to increase between 1.3 and 2.2 °C for the SSPs. The shifts were projected to be lowest for SSP1-1.9 during the 2060–2099 period, with an average of 1.3 °C, while the shift was highest (1.9 °C) for the SSP1-2.6 scenario during the 2060–2099 period.

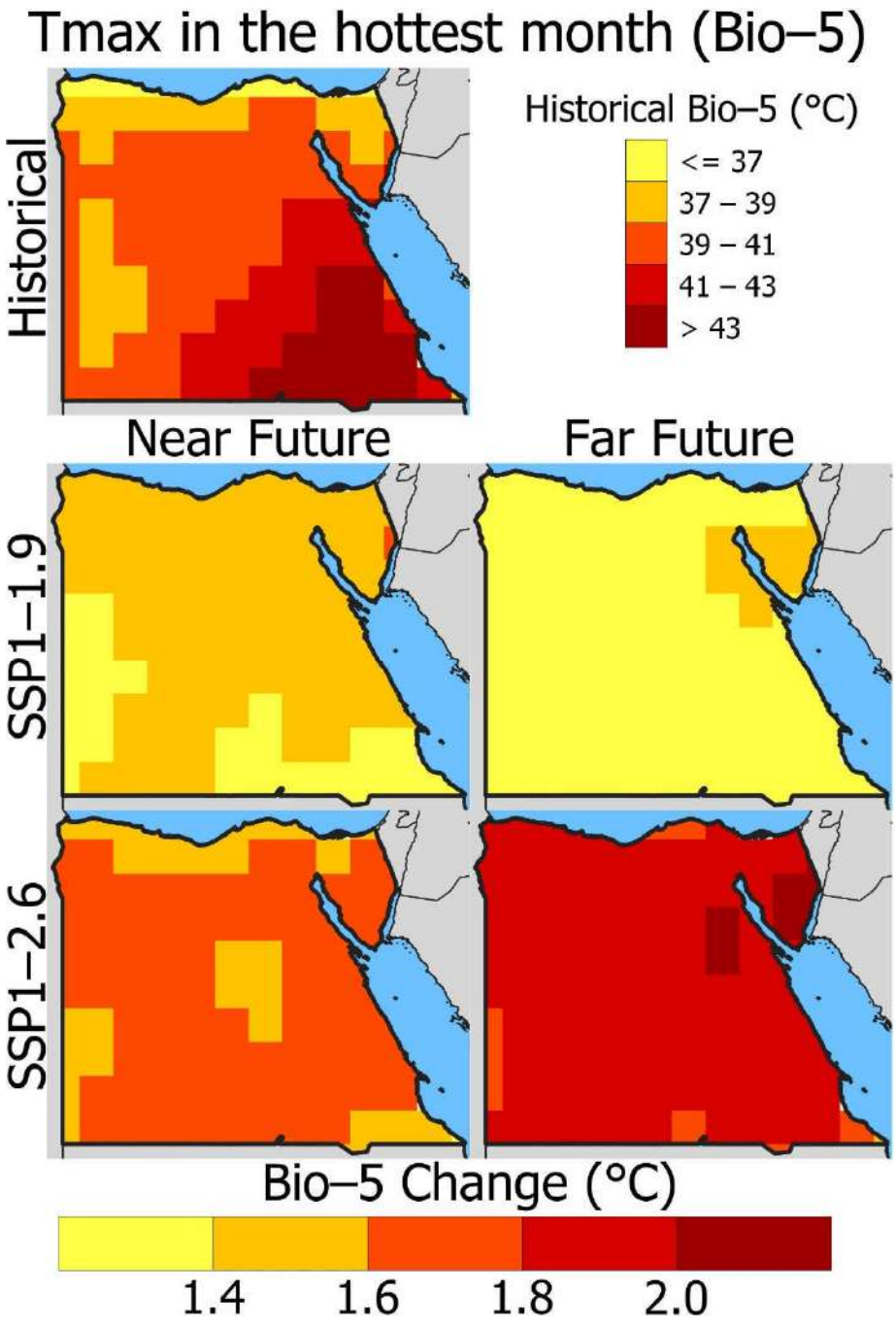

Figure 6. Same as Figure 2, but for Bio-5.

4.6. Tmin in the Coldest Month (Bio-6)

Figure 7 presents the present status and projections of the Tmin in the coldest month (Bio-6). The Bio-6 in Egypt varied from 3.5 in the southwest to 9.0 °C along the Red Sea coast. Both SSPs showed the future temperatures rising between 0.9 and 1.5 °C. The increase for SSP1-2.6 was predicted to be more than SSP1-1.9 in both future periods. The greatest

change was observed for SSP1-2.6 in 2060–2099 (1.0 °C), while the smallest change was observed for SSP1-1.9 in 2060–2099 (1.5 °C).

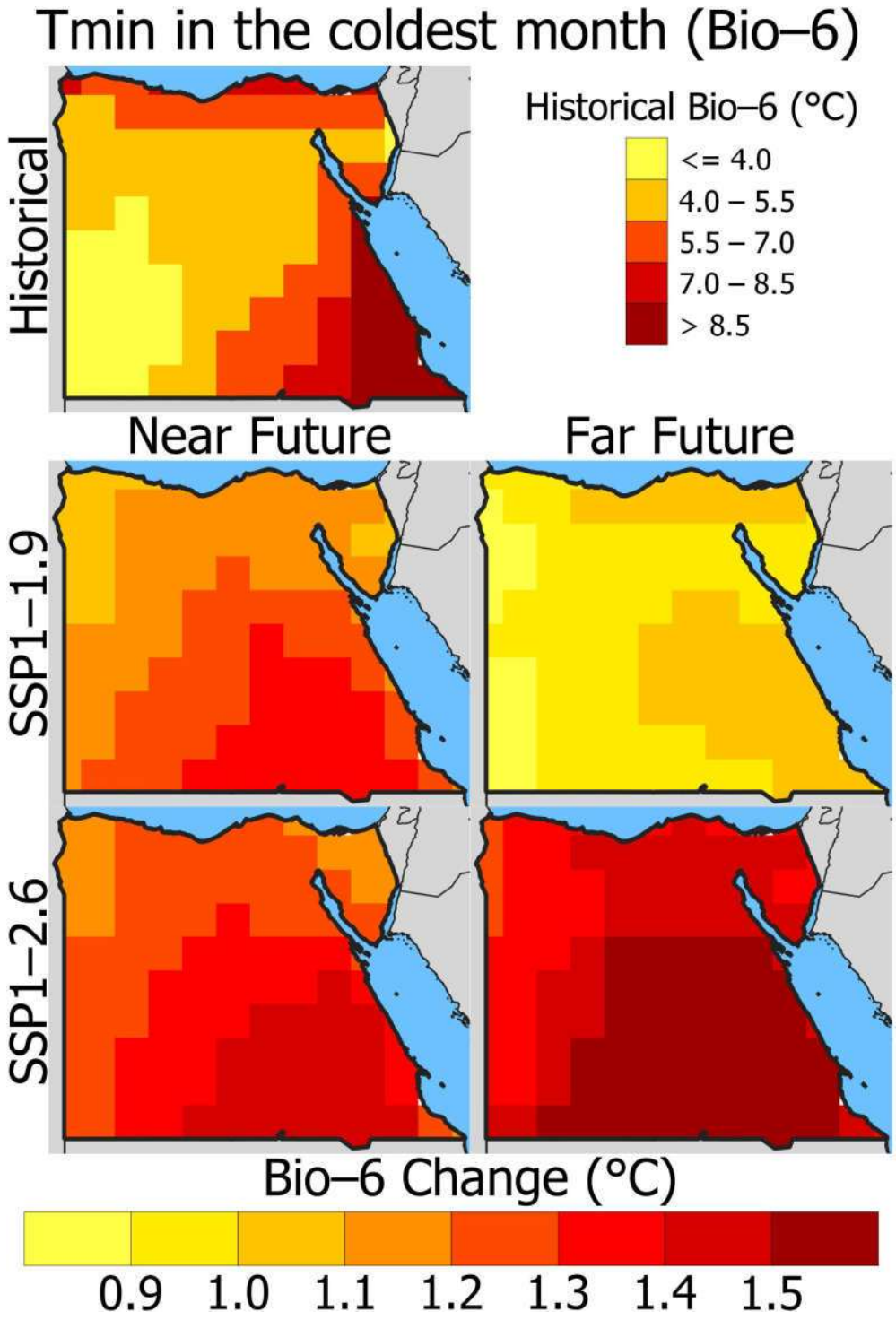

Figure 7. Same as Figure 2, but for Bio-6.

4.7. Annual Range of Temperature (Bio-7)

Bio-7 is the subtraction of Bio-6 from Bio-5. Figure 8 depicts the historical and future changes in Bio-7 in Egypt. The Figure shows that Bio-7 varied between 26.0 and 34.0 °C. The Bio-5 in most study areas was more than 33 °C, while it was low in the coastal regions. The likely shift in Bio-7 was projected to be between 0.3 and 0.4 °C. The greatest changes

were observed in northeast Egypt, and the least change was observed in the south for both scenarios.

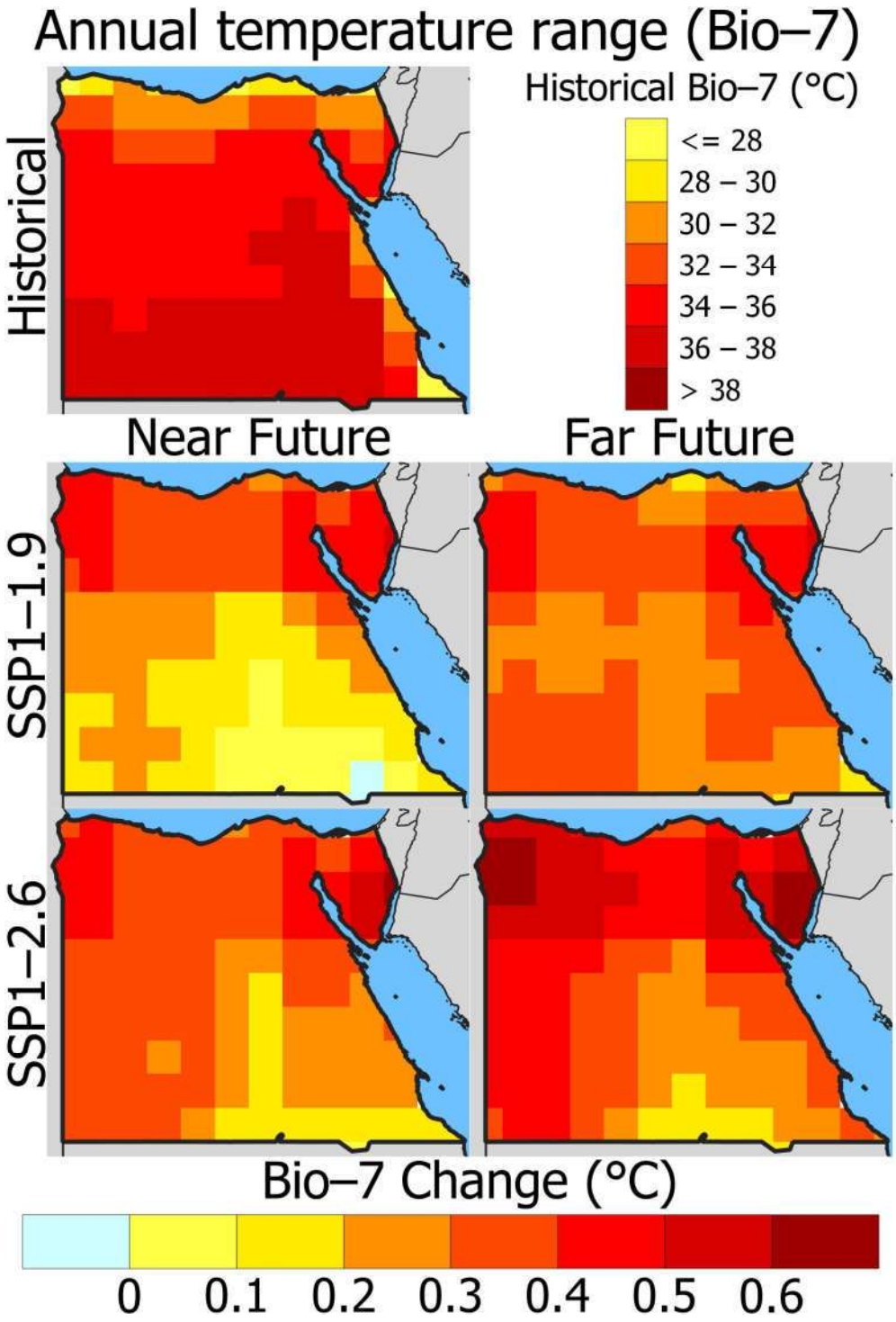

Figure 8. Same as Figure 2, but for Bio-7.

4.8. Tmean of the Wettest Quarter (Bio-8)

Due to the large diversity of Egypt's climate, the wettest quarter experiences large swings in precipitation. The wettest three months at each location were identified from the total precipitation for three successive months. Figure 9 depicts the Tmean during the wettest quarter. The Bio-8 increased from north (16 °C) to south (24 °C). Future projections

showed an uneven distribution in the change in Bio-8 across the study area for both SSPs. The increase in the Tmean was projected to be 1.5 °C for SSP1-1.9 in 2020–2059 and 1.3 °C in 2060–2099. For SSP1-2.6, the Tmean was projected to rise by 1.8 °C in 2020–2059 and by 2.2 °C in 2060–2099.

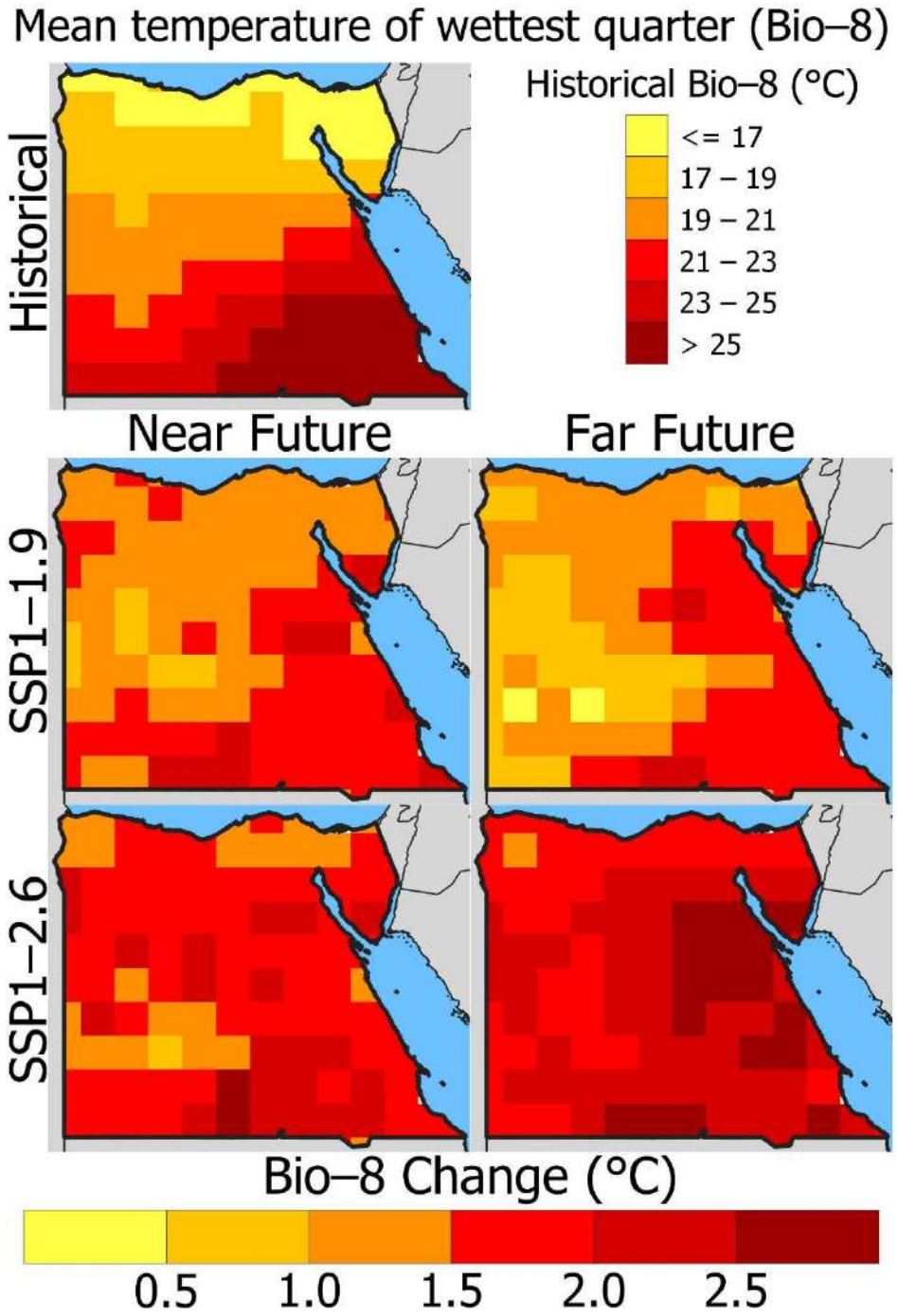

Figure 9. Same as Figure 2, but for Bio-8.

4.9. Tmean of the Driest Quarter (Bio-9)

The precipitation of three successive months was calculated in each location to find the driest period. Figure 10 illustrates the geographical variability of Bio-9 for the historical period and its likely changes for the two SSPs. The highest Bio-9 occurred in the middle and north regions (>28.5 °C), and the lowest occurred in the southwest (nearly 16.0 °C). The mean future change in Bio-9 was projected to be 1.1 °C and 1.4 °C for SSP1-1.9 and

1-2.6, respectively, representative of the 2060–2099 period. The lowest increase in Bio-9 was projected to occur in the Red Sea region, which increased by 0.2 °C for both SSPs in the 2060–2099 period. The northern part experienced the largest rise (>2 °C) for both scenarios.

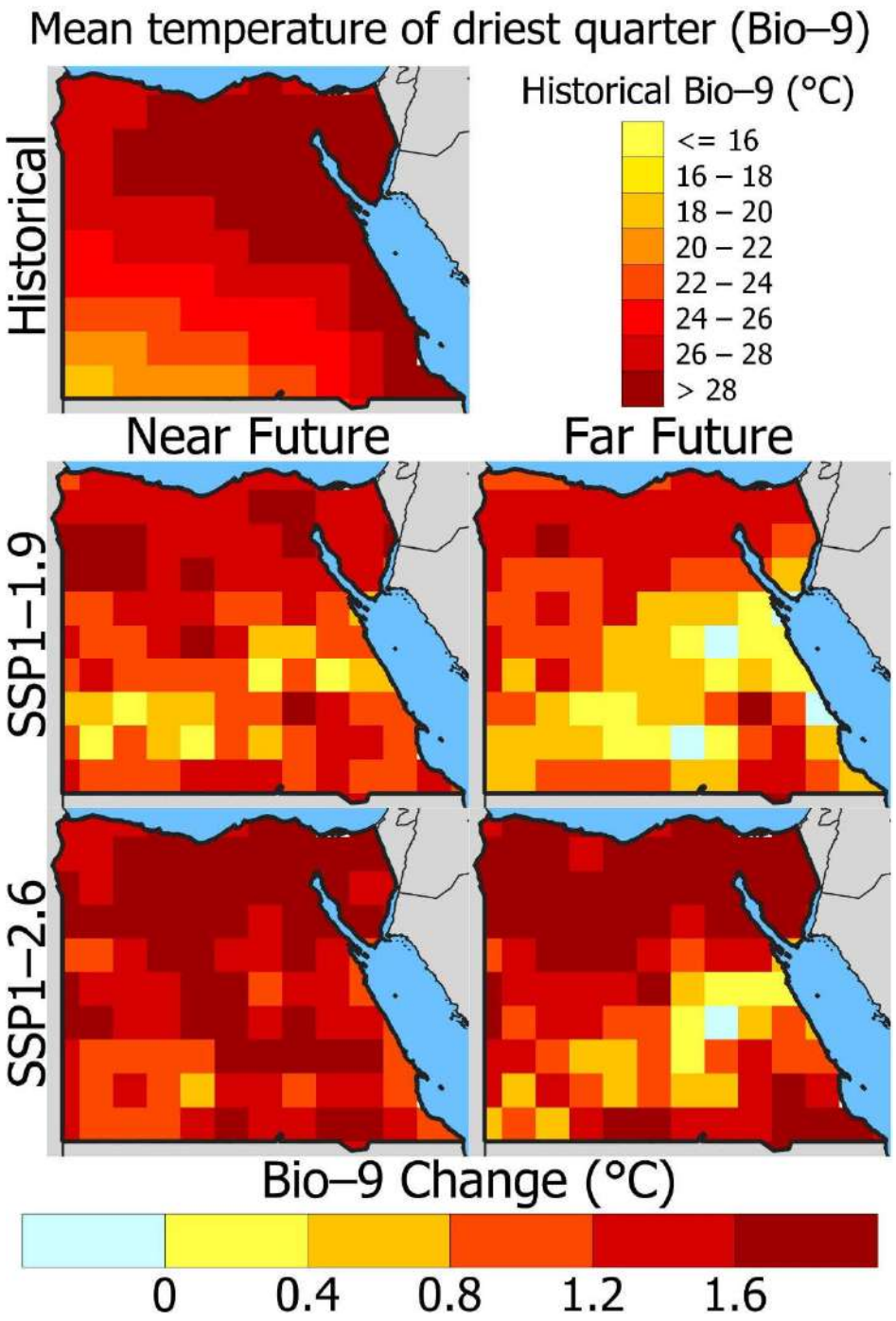

Figure 10. Same as Figure 2, but for Bio-9.

4.10. Tmean of the Warmest Quarter (Bio-10)

The Tmean for three successive months was computed to find the warmest quarter in each location. Figure 11 presents the geographical variability in Bio-10 and its future changes for the SSPs. The Bio-10 in Egypt varied between 27.0 and 33.0 °C. The Bio-10 was the greatest in the southeast and the least in the Mediterranean areas. It was projected to rise between 1.3 and 1.7 °C in the 2020–2059 period and between 1.2 and 1.5 °C in the far

future period for SSP1-1.9. The mean change in Bio-10 for SSP1-2.6 was 1.7 and 1.9 °C in the 2020–2059 and 2060–2099 periods, respectively, meaning a higher rise in Bio-10 for the SSP1-2.6 scenario than SSP1-1.9 and a higher rise in 2060–2099 compared with 2020–2059.

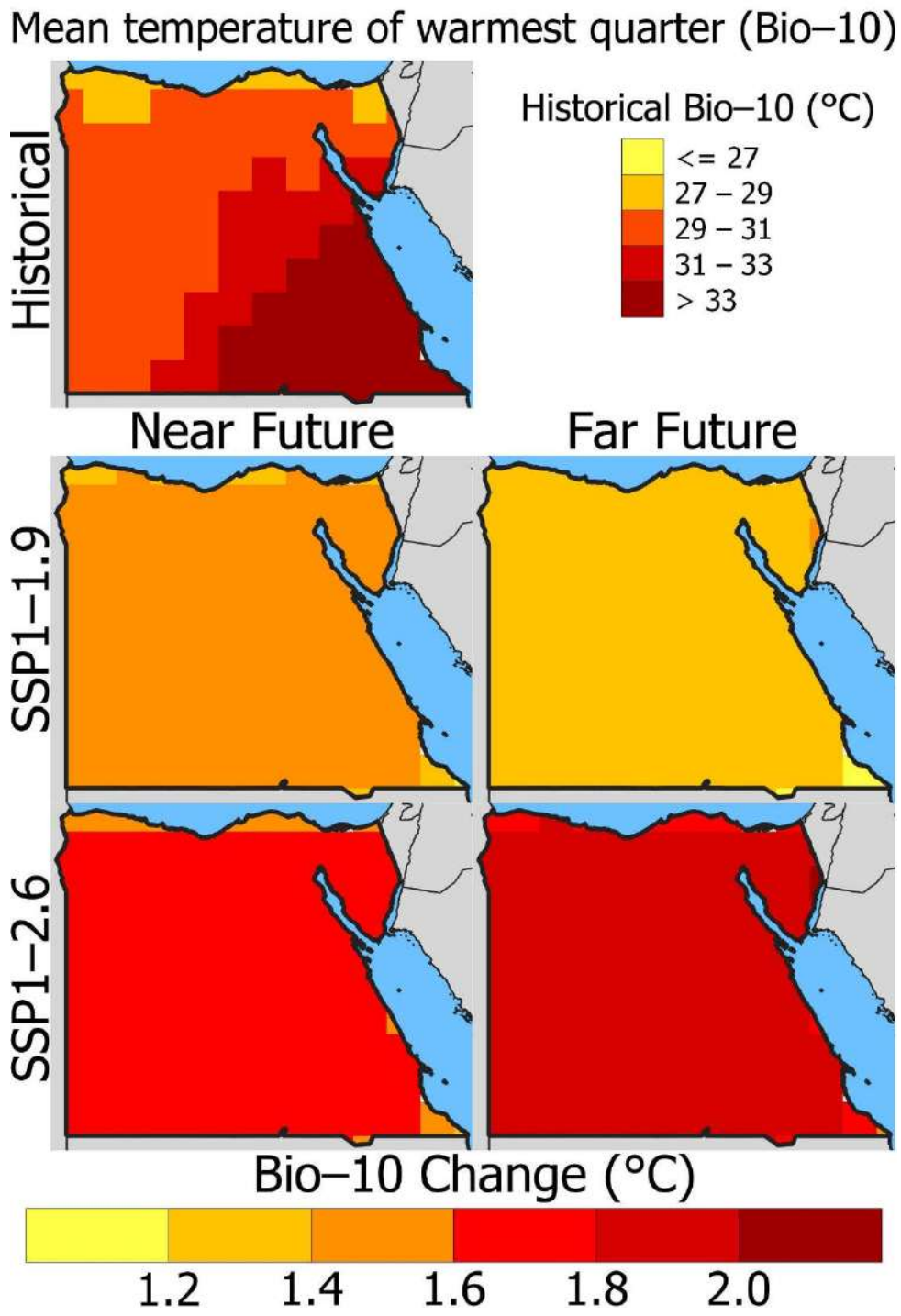

Figure 11. Same as Figure 2, but for Bio-10.

4.11. Tmean of the Coldest Quarter (Bio-11)

Figure 12 presents the geographical variability of Bio-11 for the historical period and its shifts in the two future periods for both SSPs. The Bio-11 ranged between 9.7 and 19.7 °C in Egypt. The lowest Bio-11 was in the northeast, and the highest was observed in the southeast. The Bio-11 was projected to rise for both SSPs and future periods. The lowest

mean increase was projected in 2060–2099 for SSP1-1.9 (1.0 °C). In contrast, the largest rise in the mean Bio-11 was projected in 2060–2099 for SSP1-2.6 (1.2 °C). The maximum change (>1.6 °C) was projected in the east of the study area for SSP1-2.6 in 2060–2099. The Bio-11 was projected to have a smaller increase than Bio-10, indicating more annual variation in the temperature between the coldest and warmest quarters.

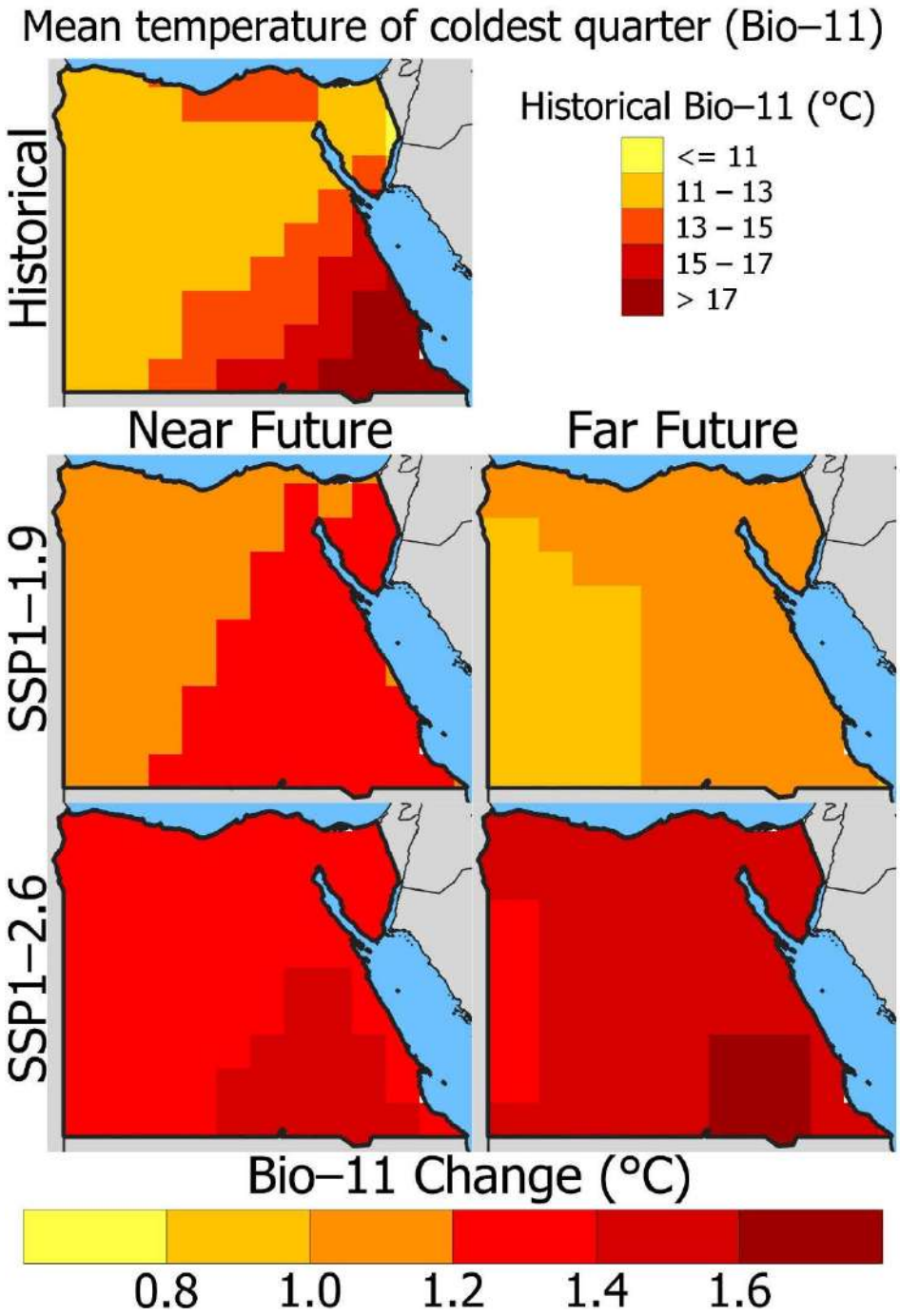

Figure 12. Same as Figure 2, but for Bio-11.

5. Discussion

The future changes of the eleven thermal bioclimatic indicators in Egypt were presented in this study. The projections were made using the MME means prepared from eight CMIP6 GCMs and the Tmax, Tmin, and precipitation for SSP1-1.9 and 1-2.6. They represent the Paris Agreement's goals of limiting the mean global warming to 1.5 and 2.0 °C.

The projected future values of the indicators were compared with the reference period to calculate their possible shifts in two future periods. This provided the likely response of the indicators to the short- and long-term changes in the global mean temperature. An increased sensitiveness of the bioenvironment to climate change was observed over the entire research region, as shown by the geographical variability of the shifts for several biothermal indicators (Table 1). Although the Paris Agreement shows that reducing carbon emissions may considerably lessen climate change's harmful consequences [50], several of the future bioclimatic indicators in Egypt would significantly change even if the goal is achieved. The high values of the bioclimatic indicators were mostly observed in the south and southeast regions of Egypt for the reference period. This indicates that the region is highly vulnerable to temperature-related extremes. The future projections showed different distributions in the change of different indicators. On the other hand, most indicators showed the greatest increase in Egypt's northern and northeastern regions. For SSP1-1.9, a rise of 1.3 °C in the annual mean temperature was projected; for SSP1-2.6, an increase of 1.5 °C was projected, notably in the southeast region of Egypt. The daily temperature variance was expected to decrease in the southeast region while increasing in the north by 0.2 °C. The hot season maximum temperatures rose by 1.3–2.2 °C, whereas the winter minimum temperatures rose by 0.9–1.5 °C.

Table 1. Summary of the results of the bioclimatic projection.

Indicator	Change	
	Increase	**Decrease**
Bio-1	Entire study area. A higher increase was projected for SSP1-2.6 in 2060–2099.	-
Bio-2	North region. A higher increase was projected in the northeast.	South region. A higher decrease was projected in the southwest.
Bio-3	-	All over the study area. The southwest has a greater projected decline.
Bio-4	-	All over the study area, with a greater decline projected in the northeast
Bio-5	All over the study area, with a greater increase projected in the northeast	-
Bio-6	All over the study area. The south and southeast have a higher projected increase.	-
Bio-7	All over the study area. The north has a higher projected increase.	-
Bio-8	All over the study area. A higher increase was projected in the east (Red Sea).	-
Bio-9	All over the study area. The north has a higher projected increase.	Red Sea region
Bio-10	All over the study area	-
Bio-11	All over the study area. The southeast has a higher projected increase.	-

This study showed that there was a higher increase in the temperature in MENA during the hottest quarter/month compared with the coldest quarter/month. These phenomena caused an increase in the annual temperature range and variations in other thermal bioclimatic indicators in the region. Cloud-free and hot weather conditions prevail in the summer of the region [51]. The elevated greenhouse gases enhance the downward component of the longwave flux, which is particularly relevant under clear skies [52]. Therefore, the temperature in the hottest month or quarter is projected to increase more in MENA than the coldest month/quarter.

Regional temperature change is often associated with evaporation, which contributes to surface cooling [53]. However, this is not the case for arid MENA regions due to the low soil heat storage capacity. The surface heat budget in an arid region is primarily controlled

by radiative cooling [54]. There is more cloud cover in the northern Mediterranean coastal region, particularly in the elevated northeastern region of Egypt. These conditions reduced the surface radiative cooling and contributed to a higher regional climate warming. The greater increase in the hottest month/quarter temperature caused a greater increase in most bioclimatic indicators in the north and northeast compared with other parts of Egypt.

The majority of economic activities in Egypt are concentrated in the north. Almost all of the population also reside in the north. The spatial pattern of the projected shifts of the bioclimates showed a higher increase in most of the indicators in the north and northeast of Egypt. The increase in temperature and greater changes in the other thermal bioclimatic indicators would affect a vast population and economy.

Few studies have projected the change in thermal bioclimatic indicators using CMIP5 GCMs [55–57]. However, none of them have inspected the changes in Egypt. Thus, comparing the results obtained in this study with others is difficult. Recently, Nashwan and Shahid [58] used an MME of CMIP5 GCMs, which showed that the Tmax rose by 1.6–4.2 °C for RCP4.5 and RCP8.5 in Egypt. In contrast, the Tmin rose by 1.3–4.4 °C. Moreover, the projected temperature rise in the cold month/season was higher than the hot month/season in Egypt [59].

The results showed a greater change in the near future period for SSP1-1.9 than the far future period for the different indicators. This is due to the integral core of the SSP1-1.9 scenario, which estimated a slight overshoot in temperature (1.6 °C) in 2050 [60]. However, reducing emissions would cool the Earth and limit global warming to roughly 1.4 °C by 2100 compared with the 1850–1900 period. Simultaneously, SSP1-2.6 showed global warming limits of about 1.8 °C [60]. The 20-year global Tmean changes and other evidence were used to show that global warming will reach 1.5 °C by 2025–2044 and 2023–2042 for the SSP1-2.6 and SSP1-1.9 scenarios, respectively [61]. The purpose of this article was to explain how the thermal bioclimatic indicators would change if the net-zero CO_2 emissions were achieved by the middle of the century in line with the Paris Agreement.

6. Conclusions

This study was conducted to examine how the regional thermal bioclimatic indicators would respond to limiting global warming by 1.5 and 2.0 °C by the end of the century compared with the pre-industrial era, according to the Paris Agreement's goals. Several GCM outputs were integrated into a mean multi-model ensemble (MME) using two shared socioeconomic paths (SSPs) (SSP1-1.9 and SSP1-2.6), which addresses the efforts made to reduce CO_2 and greenhouse gases to achieve the desired goals. The GCM MME projected diverse changes in different thermal indicators, which may affect Egypt's terrestrial habitats, flora, and fauna compositions. The ecological niche of many species is significantly limited; therefore, the shifts in the thermal bioclimatic indicators may have acute influences on Egyptian biodiversity. This is the first effort to explore the likely shift in the bioclimatic characteristics in Egypt while considering the Paris Agreement's goals. The maps plotted in this study offer helpful bioclimate information, which could be significant for the ecological climate change adaptation planning for Egypt. This study only presented the possible mean changes in the bioclimatic indicators. In the future, the uncertainty of the projected changes can be evaluated. This study employed a limited number of GCMs due to their limited availability at the time of the study. Further work can confirm these results by including other models when they become available in the future. Furthermore, the changes in the thermal bioclimatic indicators can be explored using other SSPs.

Supplementary Materials: The following supporting information can be downloaded at: https://www.mdpi.com/article/10.3390/su142013259/s1, Table S1. CMIP6 GCMs used in the study; Table S2. Description of thermal bioclimatic indicators, where Tavg is the mean temperature.

Author Contributions: Conceptualization, M.M.H.; methodology, M.M.H., T.b.I. and M.S.N.; software, M.M.H. and S.S.; validation, M.M.H. and S.S.; formal analysis, M.M.H. and M.S.N.; investigation, M.M.H.; resources, M.M.H. and T.b.I.; data curation, M.M.H.; writing—original draft preparation, M.M.H., T.b.I. and M.S.N.; writing—review and editing, M.M.H., M.S.N. and S.S.; visualization, M.M.H.; supervision, S.S. and M.S.N. All authors have read and agreed to the published version of the manuscript.

Funding: We are grateful to Universiti Teknologi Malaysia (UTM) for provide financial support to conduct this research through UTM High Impact Research Grant No. 09G07.

Institutional Review Board Statement: Not applicable.

Informed Consent Statement: Not applicable.

Data Availability Statement: Not applicable.

Conflicts of Interest: The authors declare no conflict of interest.

References

1. Hamed, M.M.; Salem, M.; Shamsuddin, N.; Tarmizi, S. Thermal bioclimatic indicators over Southeast Asia: Present status and future projection using CMIP6. *Environ. Sci. Pollut. Res.* **2022**, 1–20. [CrossRef] [PubMed]
2. Hamed, M.M.; Nashwan, M.S.; Shahid, S. Projected changes in thermal bioclimatic indicators over the Middle East and North Africa under Paris climate agreement. *Stoch. Environ. Res. Risk Assess.* **2022**, 1–18. [CrossRef]
3. O'Donnell, M.S.; Ignizio, D.A. Bioclimatic Predictors for Supporting Ecological Applications in the Conterminous United States. *U.S Geol. Surv. Data Ser. 691* **2012**, *10*, 4–9.
4. Salehie, O.; bin Ismail, T.; Hamed, M.M.; Shahid, S.; Idlan Muhammad, M.K. Projection of Hot and Cold Extremes in the Amu River Basin of Central Asia using GCMs CMIP6. *Stoch. Environ. Res. Risk Assess.* **2022**, 1–22. [CrossRef]
5. Çaliskan, O.; Türkoglu, N.; Matzarakis, A. The effects of elevation on thermal bioclimatic conditions in Uludağ (Turkey). *Atmósfera* **2013**, *26*, 45–57. [CrossRef]
6. Ragheb, A.A.; El-Darwish, I.I.; Ahmed, S. Microclimate and human comfort considerations in planning a historic urban quarter. *Int. J. Sustain. Built Environ.* **2016**, *5*, 156–167. [CrossRef]
7. Duanmu, L.; Sun, X.; Jin, Q.; Zhai, Z. Relationship between Human Thermal Comfort and Indoor Thermal Environment Parameters in Various Climatic Regions of China. *Procedia Eng.* **2017**, *205*, 2871–2878. [CrossRef]
8. Chemura, A.; Kutywayo, D.; Chidoko, P.; Mahoya, C. Bioclimatic modelling of current and projected climatic suitability of coffee (*Coffea arabica*) production in Zimbabwe. *Reg. Environ. Chang.* **2016**, *16*, 473–485. [CrossRef]
9. Salman, S.A.; Hamed, M.M.; Shahid, S.; Ahmed, K.; Sharafati, A.; Asaduzzaman, M.; Ziarh, G.F.; Ismail, T.; Chung, E.-S.; Wang, X.-J.; et al. Projecting spatiotemporal changes of precipitation and temperature in Iraq for different shared socioeconomic pathways with selected Coupled Model Intercomparison Project Phase 6. *Int. J. Climatol.* **2022**, 1–19. [CrossRef]
10. Hamed, M.M.; Nashwan, M.S.; Shahid, S. A novel selection method of CMIP6 GCMs for robust climate projection. *Int. J. Climatol.* **2022**, *42*, 4258–4272. [CrossRef]
11. Pour, S.H.; Wahab, A.K.A.; Shahid, S.; Wang, X. Spatial pattern of the unidirectional trends in thermal bioclimatic indicators in Iran. *Sustainability* **2019**, *11*, 2287. [CrossRef]
12. Salehie, O.; Hamed, M.M.; bin Ismail, T.; Shahid, S. Projection of droughts in Amu river basin for shared socioeconomic pathways CMIP6. *Theor. Appl. Climatol.* **2022**, 1–19. [CrossRef]
13. Jones, M.C.; Dye, S.R.; Fernandes, J.A.; Frölicher, T.L.; Pinnegar, J.K.; Warren, R.; Cheung, W.W.L. Predicting the Impact of Climate Change on Threatened Species in UK Waters. *PLoS ONE* **2013**, *8*, e54216. [CrossRef] [PubMed]
14. Sintayehu, D.W. Impact of climate change on biodiversity and associated key ecosystem services in Africa: A systematic review. *Ecosyst. Heal. Sustain.* **2018**, *4*, 225–239. [CrossRef]
15. Hu, X.-G.; Jin, Y.; Wang, X.-R.; Mao, J.-F.; Li, Y. Predicting Impacts of Future Climate Change on the Distribution of the Widespread Conifer Platycladus orientalis. *PLoS ONE* **2015**, *10*, e0132326. [CrossRef]
16. Waltari, E.; Schroeder, R.; McDonald, K.; Anderson, R.P.; Carnaval, A. Bioclimatic variables derived from remote sensing: Assessment and application for species distribution modelling. *Methods Ecol. Evol.* **2014**, *5*, 1033–1042. [CrossRef]
17. Molloy, S.W.; Davis, R.A.; Van Etten, E.J.B. Species distribution modelling using bioclimatic variables to determine the impacts of a changing climate on the western ringtail possum (*Pseudocheirus occidentals*; Pseudocheiridae). *Environ. Conserv.* **2014**, *41*, 176–186. [CrossRef]
18. Hamed, M.M.; Nashwan, M.S.; Shahid, S.; bin Ismail, T.; Wang, X.J.; Dewan, A.; Asaduzzaman, M. Inconsistency in historical simulations and future projections of temperature and rainfall: A comparison of CMIP5 and CMIP6 models over Southeast Asia. *Atmos. Res.* **2022**, *265*, 105927. [CrossRef]
19. Salehie, O.; Ismail, T.B.; Shahid, S.; Hamed, M.M.; Chinnasamy, P.; Wang, X. Assessment of Water Resources Availability in Amu Darya River Basin Using GRACE Data. *Water* **2022**, *14*, 533. [CrossRef]

20. Rehfeldt, G.E.; Worrall, J.J.; Marchetti, S.B.; Crookston, N.L. Adapting forest management to climate change using bioclimate models with topographic drivers. *For. Int. J. For. Res.* **2015**, *88*, 528–539. [CrossRef]
21. Ribeiro, M.M.; Roque, N.; Ribeiro, S.; Gavinhos, C.; Castanheira, I.; Quinta-Nova, L.; Albuquerque, T.; Gerassis, S. Bioclimatic modeling in the Last Glacial Maximum, Mid-Holocene and facing future climatic changes in the strawberry tree (*Arbutus unedo* L.). *PLoS ONE* **2019**, *14*, e0210062. [CrossRef] [PubMed]
22. Daham, A.; Han, D.; Matt Jolly, W.; Rico-Ramirez, M.; Marsh, A. Predicting vegetation phenology in response to climate change using bioclimatic indices in Iraq. *J. Water Clim. Chang.* **2018**, *10*, 835–851. [CrossRef]
23. Pour, S.H.; Wahab, A.K.A.; Shahid, S. Spatiotemporal changes in precipitation indicators related to bioclimate in Iran. *Theor. Appl. Climatol.* **2020**, *141*, 99–115. [CrossRef]
24. Bonan, G. A Land Surface Model (LSM Version 1.0) for Ecological, Hydrological, and Atmospheric Studies: Technical Description and User's Guide. *Natl. Cent. Atmos. Res. Boulder Color.* **1996**, *150*, 1–115.
25. Donner, L.J.; Schubert, W.H.; Somerville, R. *The Development of Atmospheric General Circulation Models: Complexity, Synthesis and Computation*; Cambridge University Press: Cambridge, UK, 2011; ISBN 0521190061.
26. McKenney, D.W.; Pedlar, J.H.; Rood, R.B.; Price, D. Revisiting projected shifts in the climate envelopes of North American trees using updated general circulation models. *Glob. Chang. Biol.* **2011**, *17*, 2720–2730. [CrossRef]
27. Eyring, V.; Bony, S.; Meehl, G.A.; Senior, C.A.; Stevens, B.; Stouffer, R.J.; Taylor, K.E. Overview of the Coupled Model Intercomparison Project Phase 6 (CMIP6) experimental design and organization. *Geosci. Model Dev.* **2016**, *9*, 1937–1958. [CrossRef]
28. Hamed, M.M.; Nashwan, M.S.; Shahid, S. Inter-comparison of Historical Simulation and Future Projection of Rainfall and Temperature by CMIP5 and CMIP6 GCMs Over Egypt. *Int. J. Climatol.* **2022**, *42*, 4316–4332. [CrossRef]
29. Taylor, K.E.; Stouffer, R.J.; Meehl, G.A. An overview of CMIP5 and the experiment design. *Bull. Am. Meteorol. Soc.* **2012**, *93*, 485–498. [CrossRef]
30. Nashwan, M.S.; Shahid, S. Future precipitation changes in Egypt under the 1.5 and 2.0 °C global warming goals using CMIP6 multimodel ensemble. *Atmos. Res.* **2022**, *265*, 105908. [CrossRef]
31. Abdelaal, M.; Fois, M.; Fenu, G.; Bacchetta, G. Biogeographical characterisation of Egypt based on environmental features and endemic vascular plants distribution. *Appl. Geogr.* **2020**, *119*, 102208. [CrossRef]
32. Younis, A.M.; Nafea, S.M. Impact of environmental conditions on the biodiversity of Mediterranean Sea lagoon, Burullus protected area, Egypt. *World Appl. Sci. J.* **2012**, *19*, 1423–1430.
33. Abbas, E.M.; Ismail, M.; El-Ganainy, A.; Ali, F.S. First DNA Barcoding-based Inventory of Suez Gulf Fishes in Egypt and its Implication for Species Diversity. *J. Ichthyol.* **2021**, *61*, 386–395. [CrossRef]
34. Farrag, M.M.S.; El-Naggar, H.A.; Abou-Mahmoud, M.M.A.; Alabssawy, A.N.; Ahmed, H.O.; Abo-Taleb, H.A.; Kostas, K. Marine biodiversity patterns off Alexandria area, southeastern Mediterranean Sea, Egypt. *Environ. Monit. Assess.* **2019**, *191*, 367. [CrossRef] [PubMed]
35. El Hadidi, M.N.; Hosni, H.A. Biodiversity in the Flora of Egypt BT. In *The Biodiversity of African Plants, Proceedings of the XIVth AETFAT Congress, Wageningen, The Netherlands, 22–27 August 1994*; van der Maesen, L.J.G., van der Burgt, X.M., van Medenbach de Rooy, J.M., Eds.; Springer Netherlands: Dordrecht, The Netherlands, 1996; pp. 785–787, ISBN 978-94-009-0285-5.
36. Ayyad, M.A.; Fakhry, A.M.; Moustafa, A.-R.A. Plant biodiversity in the Saint Catherine area of the Sinai peninsula, Egypt. *Biodivers. Conserv.* **2000**, *9*, 265–281. [CrossRef]
37. El-Sheikh, W.; El-Kenway, A.; Soliman, M. Biodiversity and Population Dynamics of Natural Enemies in the Western Desert Agro-Ecosystem, Egypt. *Egypt. Acad. J. Biol. Sci. A Entomol.* **2020**, *13*, 1–14. [CrossRef]
38. Al-Najjar, T.; Rasheed, M.; Ababneh, Z.; Ababneh, A.; Al-Omarey, H. Heavy metals pollution in sediment cores from the Gulf of Aqaba, Red Sea. *Nat. Sci.* **2011**, *3*, 775. [CrossRef]
39. El-Amier, Y.A.; El-Alfy, M.A.; Darwish, D.H.; Basiony, A.I.; Mohamedien, L.I.; El-Moselhy, K.M. Distribution and Ecological Risk Assessment of Heavy Metals in Core Sediments of Burullus Lake, Egypt. *Egypt. J. Aquat. Biol. Fish.* **2021**, *25*, 1041–1059. [CrossRef]
40. Soliman, M.M.; El-Hawagry, M.S. Impact of Urbanisation and Human Activities on Diversity and Abundance of Ulidiid Flies (Diptera: Ulidiidae) in Wadi El-Natroun, Egypt. *Afr. Entomol.* **2020**, *28*, 415–424. [CrossRef]
41. Mona, M.H.; El-Naggar, H.A.; El-Gayar, E.E.; Masood, M.F.; Mohamed, E.-S.N.E. Effect of human activities on biodiversity in Nabq Protected Area, South Sinai, Egypt. *Egypt. J. Aquat. Res.* **2019**, *45*, 33–43. [CrossRef]
42. Nashwan, M.S.; Shahid, S.; Dewan, A.; Ismail, T.; Alias, N. Performance of five high resolution satellite-based precipitation products in arid region of Egypt: An evaluation. *Atmos. Res.* **2020**, *236*, 104809. [CrossRef]
43. Hamed, M.M.; Nashwan, M.S.; Shahid, S. Performance Evaluation of Reanalysis Precipitation Products in Egypt using Fuzzy Entropy Time Series Similarity Analysis. *Int. J. Climatol.* **2021**, *41*, 5431–5446. [CrossRef]
44. Survey, B.A.; Kingdom, U.; Kingdom, U.; Survey, B.A.; Kingdom, U.; Kingdom, U. An Assessment of Recent and Future Temperature Change over the Sichuan Basin, China, Using CMIP5 Climate Models. *J. Clim.* **2017**, *30*, 6701–6722. [CrossRef]
45. Hamed, M.M.; Nashwan, M.S.; Shiru, M.S.; Shahid, S. Comparison between CMIP5 and CMIP6 Models over MENA Region Using Historical Simulations and Future Projections. *Sustainability* **2022**, *14*, 10375. [CrossRef]
46. Muhammad, M.K.I.; Shahid, S.; Hamed, M.M.; Harun, S.; Ismail, T.; Wang, X. Development of a Temperature-Based Model Using Machine Learning Algorithms for the Projection of Evapotranspiration of Peninsular Malaysia. *Water* **2022**, *14*, 2858. [CrossRef]

47. Shahid, S.; Bin Harun, S.; Katimon, A. Changes in diurnal temperature range in Bangladesh during the time period 1961–2008. *Atmos. Res.* **2012**, *118*, 260–270. [CrossRef]
48. Karoly, D.J.; Karl, B.; Stott, P.A.; Arblaster, J.M.; Meehl, G.A.; Broccoli, A.J.; Dixon, K.W. Detection of a Human Influence on North American Climate. *Science* **2003**, *302*, 1200–1203. [CrossRef]
49. Nix, H.A. A biogeographic analysis of Australian elapid snakes. *Atlas Elapid Snakes Aust.* **1986**, *7*, 4–15.
50. Chen, Y.; Liu, A.; Cheng, X. Quantifying economic impacts of climate change under nine future emission scenarios within CMIP6. *Sci. Total Environ.* **2020**, *703*, 134950. [CrossRef]
51. Lelieveld, J.; Proestos, Y.; Hadjinicolaou, P.; Tanarhte, M.; Tyrlis, E.; Zittis, G. Strongly increasing heat extremes in the Middle East and North Africa (MENA) in the 21st century. *Clim. Chang.* **2016**, *137*, 245–260. [CrossRef]
52. Vizy, E.K.; Cook, K.H.; Crétat, J.; Neupane, N. Projections of a wetter Sahel in the twenty-first century from global and regional models. *J. Clim.* **2013**, *26*, 4664–4687. [CrossRef]
53. Seneviratne, S.I.; Donat, M.G.; Pitman, A.J.; Knutti, R.; Wilby, R.L. Allowable CO_2 emissions based on regional and impact-related climate targets. *Nature* **2016**, *529*, 477–483. [CrossRef] [PubMed]
54. Zittis, G.; Hadjinicolaou, P.; Lelieveld, J. Role of soil moisture in the amplification of climate warming in the eastern Mediterranean and the Middle East. *Clim. Res.* **2014**, *59*, 27–37. [CrossRef]
55. Noce, S.; Caporaso, L.; Santini, M. A new global dataset of bioclimatic indicators. *Sci. Data* **2020**, 1–12. [CrossRef] [PubMed]
56. Navarro-Racines, C.E.; Tarapues-Montenegro, J.E.; Thornton, P.; Jarvis, A.; Ramirez-Villegas, J. CCAFS-CMIP5 Delta Method Downscaling for Monthly Averages and Bioclimatic Indices of Four RCPs. World Data Center for Climate (WDCC) at DKRZ. 2019. Available online: https://www.wdc-climate.de/ui/entry?acronym=CCAFS-CMIP5_downscaling (accessed on 25 September 2022).
57. Phillips, T.J.; Bonfils, C.J.W. Köppen bioclimatic evaluation of CMIP historical climate simulations. *Environ. Res. Lett.* **2015**, *10*, 064005. [CrossRef]
58. Nashwan, M.S.; Shahid, S. A novel framework for selecting general circulation models based on the spatial patterns of climate. *Int. J. Climatol.* **2020**, *40*, 4422–4443. [CrossRef]
59. Nashwan, M.S.; Shahid, S.; Chung, E.S. High-resolution climate projections for a densely populated mediterranean region. *Sustainability* **2020**, *12*, 3684. [CrossRef]
60. IPCC Summary for Policymakers. *Climate Change 2021: The Physical Science Basis. Contribution of Working Group I to the Sixth Assessment Report of the Intergovernmental Panel on Climate Change*; Masson-Delmotte, V., Zhai, A.P., Pirani, S.L., Connors, C., Péan, S., Berger, N., Caud, Y., Chen, L., Goldfarb, M.I., Gomis, M., et al., Eds.; Cambridge University Press: Cambridge, UK, 2021.
61. Lee, J.-Y.; Marotzke, J.; Bala, G.; Cao, L.; Corti, S.; Dunne, J.P.; Engelbrecht, F.; Fischer, E.; Fyfe, J.C.; Jones, C.; et al. Future Global Climate: Scenario-Based Projections and Near-Term Information. In *Climate Change 2021: The Physical Science Basis. Contribution of Working Group I to the Sixth Assessment Report of the Intergovernmental Panel on Climate Change*; Masson-Delmotte, V.P., Zhai, A., Pirani, S.L., Connors, C., Péan, S., Berger, N., Caud, Y.C., Eds.; Cambridge University Press: Cambridge, UK, 2021.